ORIGINAL RESEARCH

Irisin Prevents Cell Death in High Glucose via NLRP3 Inhibition

Hanwen Wei, MD; Jing Zhou, MM; Xincheng Qiu, BM; Haiyu Niu, MD; Zheng Zhang, MD; Yanjun Liu, BM; Po Bai, MM; Chao Xin, MD; Wen Wen, MM; Xiaojiong Lu, MM; Guangying Cao, MD; Taohong Hu, MD

ABSTRACT

Background • Impaired cardiac microvascular function has been implied in the pathophysiology of diabetic cardiovascular disease. However, the specific mechanism remains to be determined. Pyroptosis is a type of cell death that differs from apoptosis and autophagy. It is caused by the formation of plasma membrane pores through amino-terminal fragments of Gasdermin D (GSDMD), leading to the secretion of IL-1β and IL-18. Recent studies have shown that irisin, a myokine cleaved by the extracellular domain of FNDC5, plays a protective role in cardiovascular diseases. Here, we investigated the potential role of pyroptosis on the cardiac microvascular endothelial cells (CMECs) injury induced by high glucose (HG) and further determined the protective effect of irisin on pyroptosis.

Methods • CMECs were cultured with normal glucose (control group, 5.5 mM) and high glucose (25 mM) medium for 12, 24, and 48 h respectively. The pyroptosis of CMECs was measured by immunofluorescence staining, ELISA, and Western blot assays. Moreover, the apoptosis level was determined by flow cytometry and TUNEL staining.

Results • Our results showed that HG promoted apoptosis and pyroptosis. However, irisin reversed the increased apoptosis and pyroptosis. To investigate the underlying mechanism, we overexpressed the NLRP3 protein. We found the protective effect of irisin on apoptosis and pyroptosis was abolished by NLRP3 over-expression.

Conclusions • Our data suggest that irisin protects CMECs against apoptosis and pyroptosis, at least in part, by inhibiting NLRP3 inflammasome. (*Altern Ther Health Med.* [E-pub ahead of print.])

Hanwen Wei, MD, Associate Chief Physician; Medical College of Soochow University, Suzhou, China; Department of Cardiology, The First People's Hospital of Lanzhou, Lanzhou, China. **Hanwen Wei, MD,** Associate Chief Physician; **Jing Zhou, MM,** Attending Doctor; **Xincheng Qiu, BM,** Attending Doctor; **Zheng Zhang, MD,** Associate Chief Physician; **Yanjun Liu, BM; Po Bai, MM; Chao Xin, MD,** Attending Doctor; **Wen Wen, MM; Xiaojiong Lu, MM; Taohong Hu, MD,** Chief Physician; PLA Rocket Force Characteristic Medical Center, Beijing, China; **Haiyu Niu, MD,** Associate Chief Physician;Department of Oncology, Lanzhou University Second Hospital, Lanzhou, China; **Guangying Cao, MD,** Chief Physician; Department of Cardiology, Anshun People's Hospital, Anshun, China.

Corresponding author: Taohong Hu, MD
E-mail: Hutaohong2010@163.com
Corresponding author: Guangying Cao, MD
E-mail: caoguangying2021@163.com

INTRODUCTION

Impairment of the vascular endothelium has been observed in all forms of cardiovascular disease. Hyperglycemia causes cardiac microvascular endothelial cell (CMEC) dysfunction, which leads to the development of diabetic cardiovascular diseases.[1] Dysfunctional endothelial cells are characterized by low viability, poor migration capacity, and abnormal extracellular matrix, which eventually accelerate the progression of pathological diseases.[2] Thus, high glucose-induced poor survival has been implied in the development of diabetic vascular disorders, as well as the inhibition of cell death-induced injury is considered a therapeutic strategy for diabetes and cardiovascular diseases.

Pyroptosis, a novel programmed cell-death form associated with inflammatory mediators, is mediated by Gasdermin D (GSDMD), which is triggered by NLR family pyrin domain-containing 3 (NLRP3) inflammasome.[3] It is activated by a cleavage mediated by caspase-1 or independent caspase-1 and then releases amino-terminal Gasdermin-N and carboxy-terminal Gasdermin-C domains, which differs from apoptosis, and autophagy. The N-terminal fragment of GSDMD translocates to the plasma membrane, where it binds to phospholipids to form pores in membranes, resulting in lytic cell death with inflammatory factors secretion.[4] Previous studies have found that the roles of pyroptosis in cardiovascular disease are emerging, including myocardial infarction, ischemia–reperfusion, diabetic cardiomyopathy, and atherosclerosis.[5-7] Recently, evidence has indicated that pyroptosis occurs during microvascular endothelial cell dysfunction, such as aortic endothelial cells,[8,9] brain microvascular endothelial cells.[10] Also, accumulating studies showed that pyroptosis contributed to HG-related

microvascular endothelial cell impairment by targeting NLRP1.[11] However, how to inhibit excess pyroptosis induced by HG remains unclear.

Irisin, a myokine, is cleaved by the extracellular domain of FNDC5 which is considered a transmembrane protein with two domains (fibronectin III and carboxy-terminal).[12] Notably, evidence showed that irisin existed in the heart,[13] and was involved in regulating cardiovascular function by mediation of apoptosis and autophagy,[14-16] suggesting that irisin implies in cardioprotective effect. Recently, studies have also indicated that irisin has a protective effect on injured vascular endothelial cells induced by HG.[17] However, the effect of irisin on cardiovascular endothelial cellular pyroptosis-induced HG is unclear. Thus, we hypothesize that irisin alleviates HG-induced pyroptosis in CMECs, which may provide an optimal therapeutic target for diabetic cardiovascular diseases.

METHODS

Isolation and culture of CMECs

Isolation and culture of CMECs were performed as previously described.[18] We selected adult male C57BL/6 mice as experimental animals (from the Laboratory Animal Research Center of Rocket Army Special Medical Center of Chinese People's Liberation Army) to isolate CMECs. Before any experiment, mice were raised in a temperature-controlled facility and maintained on the background of 26±2°C and 55±15% relative humidity with a constant 12-hour light/dark cycle (light cycle, 8:00 AM to 8:00 PM), with tap water and rodent chow provided 2 weeks ad libitum. Male 8-weeks-old C57BL/6J mice were anesthetized with deep isoflurane (5%) anesthesia and then hearts were excised and rinsed with PBS supplemented with heparin. To devitalize the epicardial mesothelial cells and endocardial endothelial cells, the left ventricle was dissected and immersed in 75% ethanol for 30 seconds. The remaining tissues were then cut into 1 mm^3 and subjected to digestive juice as above. Dissociated cells were filtered and centrifuged at 1000 rpm for 5 min. The cells were resuspended in ECM complete medium (ScienCell, San Diego, CA, USA) containing 5% FBS, 1% endothelial cell growth supplement (ECGS), and 1% P/S and plated on fibrous collagen treated dishes. Primary cultures of CMECs were identified by immunofluorescence of endoglin (CD105). After confluence, media were replaced with different conditions. CMECs in control group were cultured with normal glucos medium (5.5 mM). However, CMECs in high glucose were cultured with high glucose medium (25 mM). For irisin treatment, CMECs were incubated with recombinant irisin (50 ng/mL, 100 ng/mL, 200 ng/mL) for 48 h.

Measurement of cells apoptosis

The apoptosis of CMECs was determined by flow cytometry using an Annexin V-FITC/PI Kit (Merck, Germany) according to the manufacturer's instructions.[19] In brief, CMECs were suspended in 200 μL of binding buffer. The cells were incubated with 10 μL of Annexin V solution and 5 μL propidine iodide (PI) at room temperature for 30 min respectively. CMECs were immediately analyzed on a FACSC LSR (Becton, Dickinson and Company, San Jose, CA, USA). Gating for Annexin V is FITC (maximum excitation of 488 nm and an emission of 520 nm), while PI has a maximum excitation of ~535 nm and an emission of 617 nm. Flow cytometry data were analyzed with FlowJo software (Version 10.9; Treestar, Inc., San Carlos, CA, USA).

Apoptotic CMECs were also detected by a Terminal deoxynucleotidyl transferase dUTP nick-end labeling (TUNEL) Assay Kit (In Situ Cell Death Detection Kit; Roche Diagnostics, Basel, Switzerland) according to the manufacturer's instructions and detected by confocal microscopy (Olympus Fluoview 2000, Tokyo, Japan). The total number of nuclei and the number of TUNEL-positive nuclei were determined in five random fields in each sample. The percentage of apoptotic cells was calculated by Image J software (Version 1.48; National Institutes of Health, Bethesda, MD, USA). All these assays were performed and counted in a blinded manner.

Cell viability

Cell Counting Kit-8 (CCK-8) assay was performed to determine cell viability. Briefly, cells were collected, and the culture supernatants were transformed into 10% CCK-8 fresh medium. With the background reading considered, the absorbance at 450 nm, which represents cell viability, was measured in a multimode microplate reader.[20]

Enzyme-linked immunosorbent assay (ELISA)

Cell medium supernatants were collected and stored at -20°C for the subsequent analysis of cytokines. ELISA kits, including mouse LDH (BFNE85195, Bluef Biotechnology), mouse IL-1β ELISA Kit (Abcam, ab197742, Cambridge, MA, USA), and IL-18 Mouse ELISA Kit (Thermo Fisher Scientific, KMC0181, Waltham, MA, USA) were performed following the manufacturer's instructions.

PI Staining

CMECs were stained with PI Staining Kit (E607306-0200, Sangon Biotech, Shanghai, China) according to the manufacturer's instructions and detected by confocal microscopy (Olympus Fluoview 2000, Tokyo, Japan). Cells were pretreated with different treatments (HG for 12, 24, and 48 h/Irisin). Cells were pretreated with PI (5 μL) for 30 mins. The total of nuclei WAS stained with DAPI. The total number of nuclei and the number of PI-positive nuclei were determined in five random fields. The percentage of death cells was calculated by Image J software. All these assays were performed and counted in a blinded manner.

Immunofluorescence staining

CMECs were fixed with 4% paraformaldehyde in PBS for 0.5 h, permeabilized with 0.5% Triton X-100 for 10 minutes, and blocked in 5% normal goat serum in PBS for 1 h at room temperature. Then, CMECs were probed with anti-NLRP3 antibodies, anti-ACS antibodies, and Alexa Fluor 594-conjugated goat anti-rabbit IgG secondary antibody.

After staining the cell nuclei with DAPI for 5 minutes, the immunofluorescent images were captured on a Zeiss fluorescence microscopy (Jena, Germany). Sections were imaged using a confocal microscope (Fluo-View-FV1000, Olympus, Tokyo, Japan).

RNA isolation and RT-qPCR analysis

After incubation, total RNA was extracted from cells with TRIzol (Invitrogen, Carlsbad, CA, USA), according to the manufacturer's instructions. Purified RNA (1 μg) was used for synthesizing cDNA by TransScript cDNA Synthesis SuperMix (TransGen Biotech, Beijing, China). Quantitative PCR was performed on a real-time PCR System (Eppendorf International, Hamburg, Germany) with SYBR Green PCR Master Mix. The following protocol was used for the RT-qPCR: initial activation step of 10 min at 95°C, followed by 40 cycles of 30 s at 95°C and 10 s at 52°C. The mRNA level of FNDC5 was normalized to β-actin. The RT-qPCR gene-specific primer sequences were: NLRP3: 5'-ATTACCCGCCCGAGAAAGG-3', 5'-TCGCAGCAAAGATCCACACAG-3'; β-actin: 5'-CCTTCCTTCTTGGGTATGGA-3', 5'-CTTGCTGATCCACATCTGCT-3'.

Exogenous NLRP3 over-expression vector construction and in vitro cell treatment

For over-expressions of NLRP3, the empty vector pcDNA3.1 (used as a control) and NLRP3, were purchased from Era Biotech (Shanghai, China). CMECs were infected with adenoviral vector expression NLRP3 genes for establishing cell line stable expression of GFP-NLRP3. All inserted genes were sequenced. Adenoviral vectors were generated and purified as described. Stable expression of GFP-NLRP3 cells was stimulated by irisin at 37°C. At the end of each experiment, the cells and culture medium were then collected for further study.

Western blot analysis

The proteins (50 μg/lane) extracted from cardiomyocytes were fractionated by sodium dodecyl sulfate-polyacrylamide gel electrophoresis (SDS-PAGE) and blotted to polyvinylidene fluoride (PVDF) membranes (Millipore, Billerica, MA, USA). Membranes were blocked for 1 h using 5% nonfat milk. Then, the whole-cell extracts were probed overnight with the following primary antibodies at 4°C: Cleaved caspase-3(1:500 dilution), Cleaved caspase-1 (1:500 dilution), NLRP3 (1:500 dilution), ACS (1:500 dilution), GSDMD (1:500 dilution), and β-actin (1:1000 dilution). After incubation with the primary antibodies, membranes were incubated with secondary antibodies for 1 h. The protein bands were quantified by measuring the band intensity in each group.

Statistical analysis

The data analysis was performed with GraphPad Prism software (Version 8.0; La Jolla, CA, USA). All quantitative data are expressed as the means ± SEM. The Shapiro–Wilk normality test was performed to determine the normality of the data distribution. Differences between two groups or multiple groups were analyzed using the Student's t-test and ANOVA, respectively. Bonferroni testing was performed to determine post hoc testing. A $P < .05$ was considered significant.

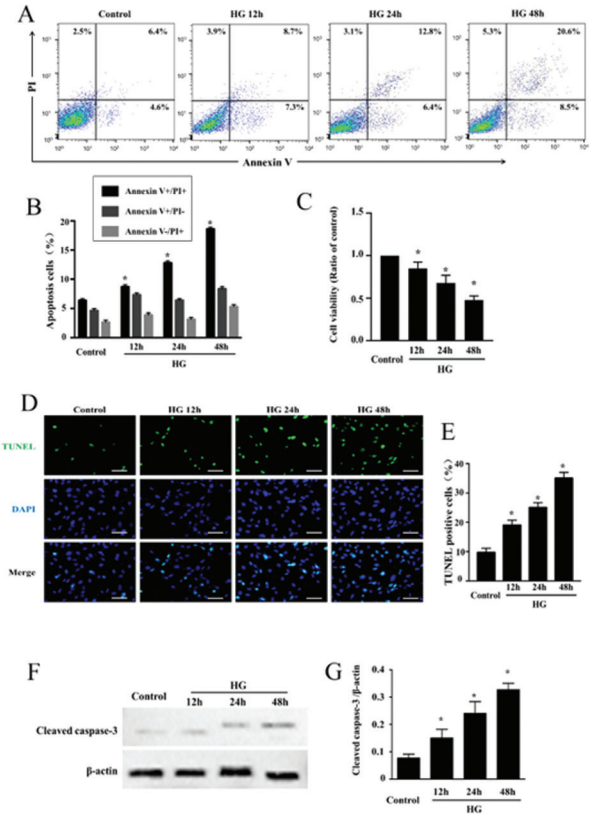

Figure 1. High glucose induces apoptosis of CMECs. (A) Representative results of the FACS analysis in CMECs under high glucose for 12, 24, and 48 h. Viable cells: Annexin V^-/PI^-; Early apoptosis: Annexin V^+/PI^-; late apoptosis: V^+/PI^+; Necrotic: V^-/PI^+. (B) Quantification of the apoptotic CMECs (n = 5, $^*P < .05$). (C) CCK-8 assay under different treatments (n = 5, $^*P < .05$). (D) Representative TUNEL staining imaging of CMECs under high glucose for 12, 24, and 48 h (scale bars 20 μm). (E) Quantification of TUNEL positive CMECs in all groups (n = 5, $^*P < .05$). (F) Representative Western blots of cleaved caspase-3 in each group. (G) Semi-quantification of Cleaved caspase 3 expression. Data are expressed as the means ± SEM; n = 5; $^*P < .05$.

RESULTS

HG stress increased apoptosis in CMECs

To analyze the apoptosis induced by HG stress in CMECs, we performed flow cytometry, TUNEL staining, and Western blot assays. Annexin V is considered a marker for early apoptosis. Early apoptotic cells will only take up Annexin V stain while remaining PI negative. The late-stage apoptotic and necrotic cells will be positive for both Annexin V and PI. The representative flow cytometry results indicated that the percentage of early-stage apoptotic CMECs with HG stimuli for 12–48 h was significantly increased than that in the control

Figure 2. High glucose induces pyroptosis of CMECs. (A) Staining the cells with PI and analyzing the cells under a microscope (scale bars 20 μm). (B) Quantification of the pyroptotic CMECs (n = 5, *$P < .05$). (D) Immunofluorescence staining with NLRP3 and ACS antibodies by confocal microscope (scale bars 20 μm). (E) Western blot assay of NLRP3, ACS, GSDMD, GSDMD-N, and Cleaved-caspase-1. Semi-quantification of NLRP3 (H), ACS (I), GSDMD-N (J), Cleaved caspase 1 (K) expression. Representative ELISA assay of LDH (C), IL-1β (F), IL-18 (G). Data are expressed as the means ± SEM; n = 5; *$P < .05$.

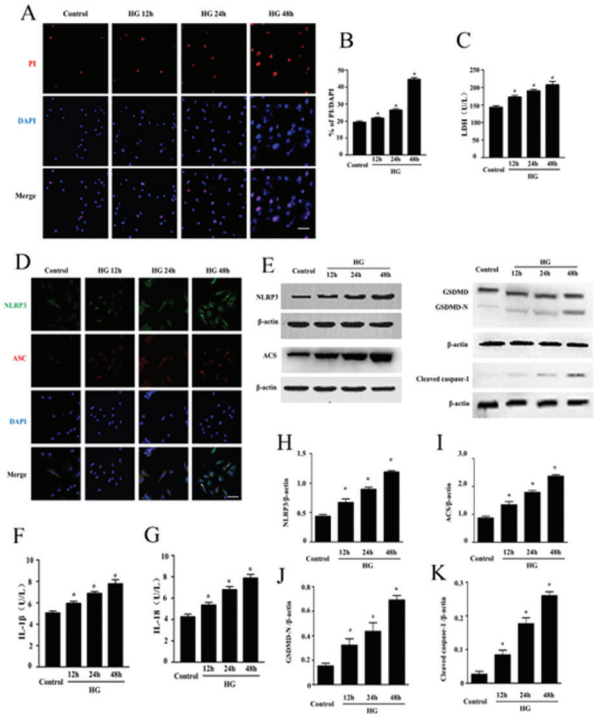

Figure 3. The apoptosis and pyrotosis after Administration of CMECs with different concentrations of irisin. (A) TUNEL staining imaging of CMECs (scale bars 20 μm). (B) PI staining of cells under a microscope (scale bars 20 μm). (C) Quantification of TUNEL positive CMECs (n = 5, *$P < .05$). (D) Quantification of the PI-positive CMECs (n = 5, *$P < .05$). (E) Representative CCK-8 assay (n=5, *$P < .05$). Data are expressed as the means ± SEM; n = 5; *$P < .05$.

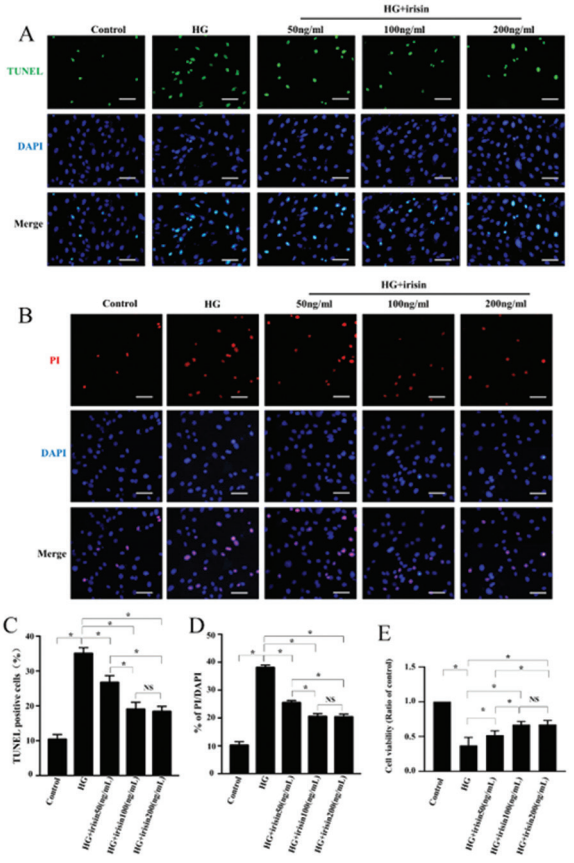

group (F = 5.32, $P = .014$, Figure 1A, 1B). The representative CCK-8 assay demonstrated that high glucose decreased the viability of CMECs (F = 5.23, $P = .013$, Figure 1C). Meanwhile, TUNEL results revealed that the numbers of all nuclear in all groups were 96.34±2.15/ HP, 95.78±1.78/ HP, 98.23±2.03/ HP, and 97.23±1.86/HP (F = 1.49, $P = .25$). However, the numbers of TUNEL-positive cells under HG for 12–48 h were 16.34±1.32/ HP, 25.22±1.83/HP, and 37.83±2.31/HP, significantly increasing than the control group (9.21±1.04, F = 108.4, $P < .0001$). Furthermore, the quantitative analysis showed that TUNEL-positive cells under HG for 12–48 h were 19.23±1.73%, 25.21±1.32%, and 35.04±1.16%, significantly increased than that in normal glucose (9.67±1.45%, F = 276.8, $P < .0001$, Figure 1D, 1E). The active caspase-3 represents the apoptotic process. Thus, we further detected the expression of caspase-3. The representative Western blot results and semi-quantitative analysis showed that high glucose upregulated the expression of cleaved caspase-3 compared with that in the control group (Figure 1F, 1G). Taken together, our results indicated that HG increased apoptosis in CMECs time-dependently.

HG stress increased Pyroptosis in CMECs

To understand the effect of HG stress on pyroptosis, we performed PI staining. As shown in Figures 2A and 2B, the numbers of all nuclear in all groups were 26.74±1.98/ HP, 29.23±1.83/ HP, 28.21±1.08/ HP, and 27.34±1.32/ HP (F = 2.31, $P = .12$). However, the numbers of PI-positive cells under HG for 12–48 h were 7.53±0.76 / HP, 8.33±1.03/ HP, and 16.19±1.21/ HP, significantly increased than the control group (F = 148.7, $P < .0001$), suggesting that PI-positive cells were increased after administration to HG. Inflammasome, including NLRP3, ACS, and caspase-1, contributes to GSDMD-related pyroptosis with the secretion of LDH and inflammatory factors, such as IL-18, and IL-1β. Therefore, we detected NLRP3 and ACS with immunofluorescent staining and Western blot assays. The results indicated that HG increased the expressions of NLRP3 and ACS compared with normal glucose (Figure 2D). Meanwhile, the expressions of cleaved caspase-1 and GSDMD-N were increased under HG treatment (Figure 2E, 2H, 2I, 2J, 2K). Furthermore, ELISA assays were performed to detect the expressions of LDH,

Figure 4. Irisin decreased HG-induced apoptosis. (A) The results of the FACS analysis in CMECs under irisin treatment. (B) Quantification of the apoptotic CMECs (n = 5, *P < .05). (C) Representative CCK-8 assay (n = 5, *P < .05). (D) TUNEL staining imaging of CMECs (scale bars 20 μm). (E) Quantification of apoptotic CMECs in all groups (n = 5, *P < .05). (F) Western blots of cleaved caspase-3 in each group. (G) Semi-quantification of Cleaved caspase 3 expression. Data are expressed as the means ± SEM; n = 5; *P < .05.

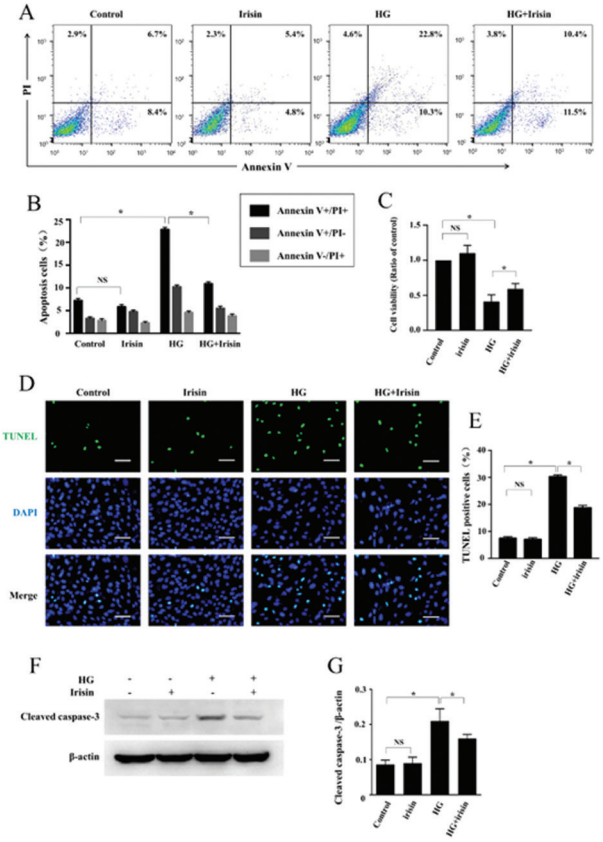

Figure 5. Irisin reduced HG-induced pyroptosis of CMECs. (A) Representative PI staining under a microscope (scale bars 20 μm). (B) Quantification of the pyroptotic CMECs (n = 5, *P < .05). (D) Representative immunofluorescence staining with NLRP3 and ACS antibodies (scale bars 20 μm). (E) Western blot assay of NLRP3, ACS, GSDMD, GSDMD-N, and Cleaved-caspase-1. Semi-quantification of NLRP3 (H), ACS (I), GSDMD-N (J), Cleaved caspase 1 (K) expression. ELISA assay of LDH (C), IL-1β (F), IL-18(G). Data are expressed as the means ± SEM; n = 5; *P < .05.

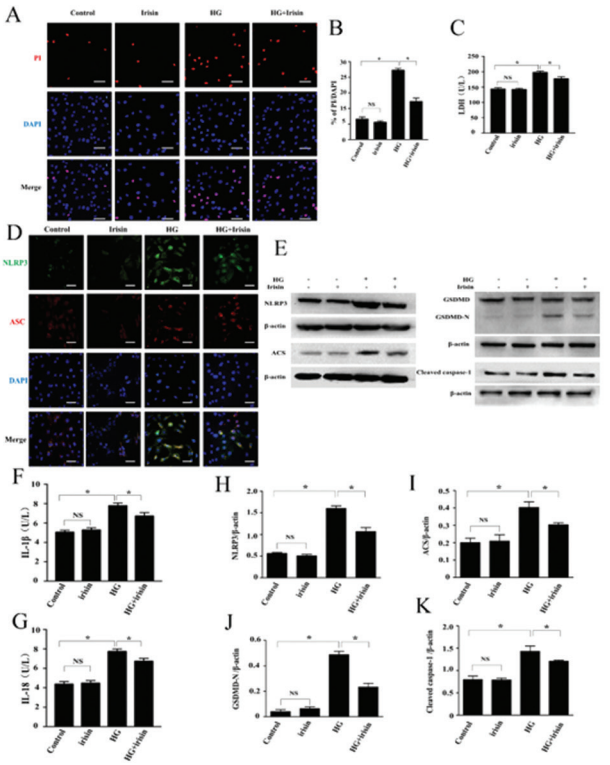

IL-18, and IL-1β. The ELISA results demonstrated that HG promoted the secretion of LDH, IL-18, andIL-1β (Figure 2C, 2F-2G). These data indicated that HG stress-activated pyroptosis. In addition, as shown in Figure 1 and Figure 2, HG for 48 h which significantly induced apoptosis and pyroptosis, was used in further study.

Irisin improved HG-induced apoptosis in CMECs

Different concentrations of irisin were administrated to CMECs to screen the appropriate concentration. The results of TUNEL, PI stain, and CCK-8 assay showed that 100 ng/mL and 200 ng/mL irisin significantly reduced apoptosis and pyroptosis compared with 50 ng/mL irisin, but no significance among them (Figure 3A-3E). Therefore, 100 ng/mL irisin was used to perform further study.

To explore the protective effect of irisin, flow cytometry, TUNEL staining, and Western blot assay were performed to detect apoptosis in CMECs. The representative flow cytometry results indicated that irisin reduced the percentage of early-stage apoptotic CMECs with HG (t = 7.61, P = .0015, Figure 4A, 4B). The CCK-8 assay demonstrated that irisin reversed the low viability of CMECs (t = 5.33, P = .005, Figure 4C). Meanwhile, TUNEL stain results and the quantitative analysis showed that apoptosis of CMECs was repressed after irisin treatment (t = 3.13, P = .013, Figure 4D-4E). Meanwhile, our Western blot results and semi-quantitative analysis showed that irisin down-regulated the upregulated expression of cleaved caspase-3 compared with that in the HG group (t = 4.27, P = .008, Figure 4F, 4G). These results suggested that irisin improved HG-induced increased apoptosis in CMECs.

Irisin ameliorates HG-induced pyroptosis in CMECs

To understand the effect of irisin on pyroptosis, we performed PI staining. In Figures 5A and 5B, PI-positive cells were decreased after administration of irisin (t = 5.81, P = .004). Furthermore, we detected NLRP3 and ACS with immunofluorescent staining and Western blot. These results and semi-quantitative analyses showed that irisin suppressed the

Figure 6. NLRP3-OV reversed the protective effect on HG-induced apoptosis. (A) The results of the FACS analysis in CMECs under various treatments. (B) Quantification of apoptotic CMECs in all groups (n = 5, *P < .05). (C) TUNEL staining imaging of CMECs (scale bars 20 μm). (D) Quantification of apoptotic CMECs in all groups (n = 5, *P < .05). (E) Western blots of cleaved caspase-3. (F) Semi-quantification of Cleaved caspase 3 expression. Data are expressed as the means ± SEM; n = 5; *P < .05.

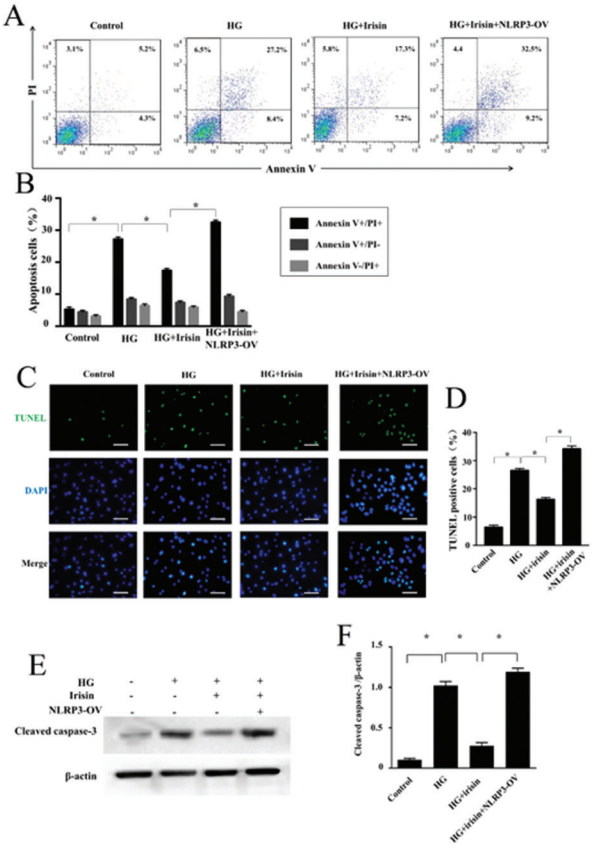

Figure 7. NLRP3-OV reversed the protective effect on HG-induced pyroptosis. (A) PI staining under a microscope (scale bars 20 μm). (B) Quantification of the pyroptotic CMECs (n=5, *P < .05). (C) Immunofluorescence staining with NLRP3 and ACS antibodies (scale bars 20 μm). (D) Western blot assay of NLRP3, ACS, GSDMD, GSDMD-N, and Cleaved-caspase-1 in each group. Semi-quantification of NLRP3 (E), ACS (F), GSDMD-N (G), Cleaved caspase 1 (H) expression. Data are expressed as the means ± SEM; n = 5; *P < .05.

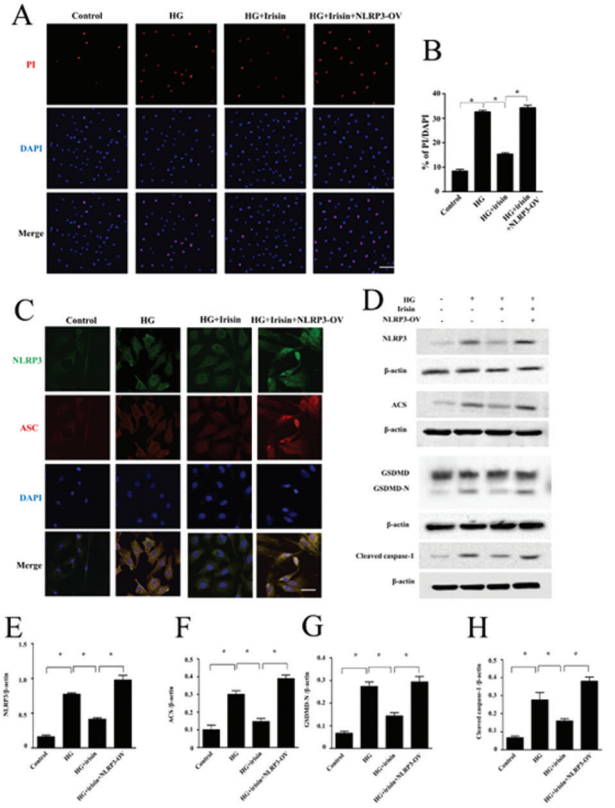

expression of NLRP3 and ACS compared with high glucose (Figure 5D). Meanwhile, the expressions of cleaved caspase-1 and GSDMD-N were decreased under irisin treatment (Figure 5E, 5H-5K). Furthermore, to investigate the effect of irisin on, LDH, IL-18, andIL-1β, an ELISA assay was performed. These results demonstrated that the increased secretion of LDH, IL-18, andIL-1β was repressed after administration of irisin (Figure 5C, 5F-5G). Taken together, these data indicated that irisin ameliorated HG-induced pyroptosis of CMECs.

Irisin ameliorates HG-induced apoptosis and pyroptosis by repressing NLRP3 inflammasome

To further understand the underlying mechanism, we over-expressed the NLRP3 protein (Supplemental Figure 1). The flow cytometry result indicated that the percentage of early-stage apoptotic CMECs was elevated after over-expression treatment (t = 4.98, P = .006, Figure 6A, 6B). TUNEL staining assay results indicated that TUNEL positive CMECs under over-expression treatment was 34.17±0.61%, significantly increased under that of Irisin treatment (16.23±0.67%, t = 44.27, P < .0001, Figure 6C, 6D). Meanwhile, Western blot results showed the upregulated expression of cleaved caspase-3 in the NLRP3-OV group (Figure 6E-6F). These results suggested that NLRP3-OV increased apoptosis in CMECs.

Meanwhile, we performed PI staining to detect pyroptosis. As shown in Figures 7A and 7B, PI-positive cells were increased after administration to over-expression (t = 5.81, P = .004). Furthermore, immunofluorescent staining and Western blot showed a high expression level of NLRP3 and ACS compared with irisin treatment (t = 3.12, P = .012, Figure 7C-7F). Meanwhile, the expressions of cleaved caspase-1 and GSDMD-N were upregulated (t = 22.57, P < .0001, Figure 7D, 7G-7H). These data indicated that NLRP3-OV promoted pyroptosis of CMECs with irisin treatment. Taken together, these data showed that irisin played a protective role in apoptosis and pyroptosis, at least partly, by inhibiting NLRP3 inflammasome.

DISCUSSION

Pyroptosis is a novel programmed cell death that is triggered by NLRP3 inflammasome activation which results in inflammatory factors secretion. Irisin is a myokine that plays a protective effect on improving cell death. However, the effect of irisin on CMECs death, including pyroptosis and apoptosis induced by high glucose is poorly understood. In the present study, our data suggested that HG stress increased CMECs death including apoptosis and pyroptosis. Meanwhile, HG activated NLRP3 inflammasome and inflammatory factors secretion. Reversely, irisin decreased apoptosis and pyroptosis, inactivated NLRP3 inflammasome, and reduced inflammatory factors secretion. Importantly, over-expression of NLRP3 suppressed the protective effect of irisin on CMECs injuries. Taken together, our data suggested that irisin ameliorates apoptosis and pyroptosis, by repressing the activation of NLRP3 inflammasome (Figure 8).

It has been reported that diabetic microvascular injury plays an important role in cardiac dysfunction.[21] Endothelial cells, considered as an important modulator in vascular homeostasis, play a critical role in inhibiting vascular inflammation and oxidative stress and are regulated by various paracrine factors. Endothelial dysfunction is a classical feature and predictor of cardiovascular diseases.[22] Myocardial microvascular dysfunction is an early feature of DM and is now recognized as a potential contributor to CVD risk in this population. Some anti-diabetic medication increases cardiovascular risk, so safer drug targets are urgently needed to improve cardiovascular disease in diabetes.[23] Therefore, improving cardiac microvascular dysfunction is essential for maintaining circulatory homeostasis and cardiac physiological function.[24] In the present study, we found that HG reduced the CMECs' viability. Moreover, elevating CMECs survivals is important for diabetic microvascular injury.

Pyroptosis, a type of lytic programmed cell-death form associated with inflammatory mediators, which is mediated by GSDMD, is an important natural immune response.[3] Pyroptosis is induced by activation of NLRP3 inflammasome and triggered by caspase-1, which controls GSDMD and activates inflammatory factors IL-1β and IL-18.[4,24] Studies have shown that pyroptosis plays an important role in many diseases such as diabetes, obesity, atherosclerosis, and so on.[26-28] Thus, in our study, we explore whether caspase-1/GSDMD dependent pyroptosis plays a significant role in microvascular injury induced by HG. We identified that caspase-1, GSDMD, ACS, and IL-1β, IL-18 levels were up-regulated in CMECs during HG stress, suggesting that caspase-1 mediated pyroptosis indeed plays a pivotal role in diabetic cardiac microvascular injury. Thus, targeting pyroptosis may be a potential strategy for limiting CMECs dysfunction.

Recently, irisin has been considered as a myokine that is cleaved by the extracellular domain of FNDC5[12], involved in regulating cardiovascular function.[14,15] Accumulating studies showed that irisin has implied in reduced apoptosis,[29] and pyroptosis.[30] Interestingly, irisin also has a protective effect on injured vascular endothelial cells induced by HG.[17] However, the effect of irisin on cardiovascular endothelial cellular dysfunction such as pyroptosis and apoptosis induced HG is not fully clarified. In the present study, we found that irisin reduced TUNEL-positive cells and the high expression levels of caspase-3, suggesting that irisin suppressed apoptosis induced by HG stimuli. In addition, we found that irisin reduced PI-positive cells and the expressions of caspase-1, GSDMD, ACS, and IL-1β, IL-18, indicating that irisin also repressed HG-induced pyroptosis.

Figure 8. A proposed mechanism that irisin ameliorates apoptosis and pyroptosis, by repressing activation of NLRP3 inflammasome.

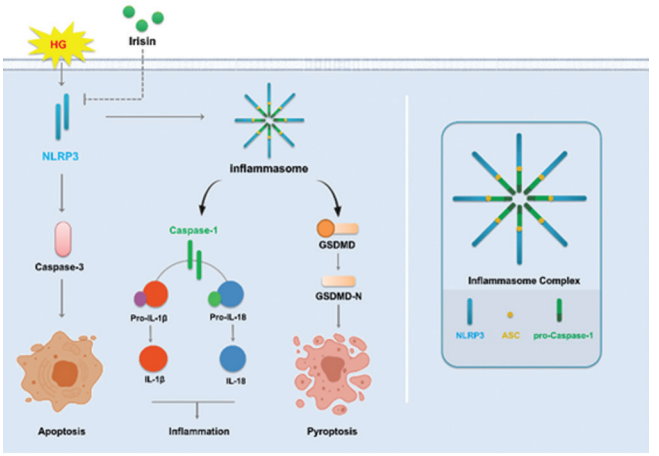

To elucidate the underlying mechanisms, we investigated the effects of irisin on the NLRP3 inflammasome. Inflammasome, including NLRP3, ACS, and caspase-1,[31] contributes to pyroptosis.[32] Our results showed that irisin can attenuate the high glucose injury of CMEC, and reduce the expressions of NLRP3 and ACS, suggesting that irisin can inhibit the activation of NLRP3 inflammasome under high glucose conditions. Therefore, we hypothesized that irisin might play a protective role in CMEC by inhibiting NLRP3 inflammasome activation. To investigate this hypothesis, we activated the inflammasome through NLRP3 over-expression. Interestingly, the protective effects of irisin were abolished by NLRP3 over-expression. Previous studies have indicated that irisin acts potentially beneficial cardiac effects by suppressing inflammation.[16,33]

Although our study bears some significance, there are some limitations. Firstly, in *vitro,* HG treatment was an artificial model that failed to fully mimic the pathological changes in diabetes patients. we will explore the detailed mechanisms of endothelial damage in diabetes other than direct damage from high glucose in our following studies. Secondly, the detailed molecular mechanism between irisin and NLRP3 was not clarified completely. PKM2, a key enzyme of glycolysis, can promote the expression of NLRP3. Whether Irisin can regulate NLRP3 through PKM2 needs further investigation.

CONCLUSION

In summary, repairing cardiac microvascular dysfunction is essential for maintaining circulatory homeostasis and cardiac physiological function, and can reduce cardiovascular disease risk in the population with diabetes. Here, we investigated the potential role of pyroptosis on the CMECs injury induced by HG and further determined the protective effect of irisin on pyroptosis. Our results indicate that irisin protects against apoptosis and pyroptosis induced by high glucose, probably by suppressing the activation of NLRP3 inflammasome. This indicates that irisin may be a promising target for improving regulated CMECs death resulting from diabetes mellitus.

ETHICAL COMPLIANCE

This study was approved by the Animal Use and Care Committee of PLA Rocket Force Characteristic Medical Center (ID: 5034), Beijing, China.

STATEMENT OF HUMAN AND ANIMAL RIGHTS

All of the experimental procedures involving animals were conducted by the Institutional Animal Care guidelines of PLA Rocket Force Characteristic Medical Center, and approved by the Animal Use and Care Committee of PLA Rocket Force Characteristic Medical Center, Beijing, China.

STATEMENT OF INFORMED CONSENT

There are no human subjects in this article and informed consent is not applicable.

AUTHORS' CONTRIBUTIONS

HWW, JZ and XCQ contributed equally. HWW, XYF, ZZ, and THH designed the study, drafted the manuscript, and approved its final version. HYN, GYC, ZTJ, CX, CRZ, CX, YFL, and XL acquired the data, revised the intellectual content, and approved the final version. ZZ and THH are responsible for the integrity of this work. All authors read and approved the final manuscript.

DECLARATION OF CONFLICTING INTERESTS

The author(s) declared no potential conflicts of interest concerning the research, authorship, and/or publication of this article.

DATA AVAILABILITY STATEMENTS

The datasets generated during and/or analyzed during the current study are available from the corresponding author upon reasonable request.

FUNDING

The study was funded by the Lanzhou Talents Innovation and Entrepreneurship Project (2019-RC-71), the Gansu Province Science and Technology Plan Project (23JRRA0991), and the Cuiying Scientific and Technological Innovation Program of Lanzhou University Second Hospital (CY2022-QN-A07).

REFERENCE

1. Jin Y, Hong HS, Son Y; Substance P enhances mesenchymal stem cells-mediated immune modulation. *Cytokine*. 2015;71(2):145-153. . 10. 003 doi:10.1016/j.cyto.2014.10.003
2. Kim DY, Piao J, Hong HS. Substance-P Inhibits Cardiac Microvascular Endothelial Dysfunction Caused by High Glucose-Induced Oxidative Stress. *Antioxidants*. 2021;10(7):1084. doi:10.3390/antiox10071084
3. Evavold CL, Hafner-Bratkovič I, Devant P, et al. Control of gasdermin D oligomerization and pyroptosis by the Ragulator-Rag-mTORC1 pathway. *Cell*. 2021;184(17):4495-4511. e19. doi:10.1016/j.cell.2021.06.028
4. He X, Fan X, Bai B, Lu N, Zhang S, Zhang L. Pyroptosis is a critical immune-inflammatory response involved in atherosclerosis. *Pharmacol Res*. 2021;165:105447. doi:10.1016/j.phrs.2021.105447
5. Jia C, Chen H, Zhang J, et al. Role of pyroptosis in cardiovascular diseases. *Int Immunopharmacol*. 2019;67:311-318. doi:10.1016/j.intimp.2018.12.028
6. Wu X, Iroegbu CD, Peng J, Guo J, Yang J, Fan C. Cell Death and Exosomes Regulation After Myocardial Infarction and Ischemia-Reperfusion. *Front Cell Dev Biol*. 2021;9:673677. doi:10.3389/fcell.2021.673677
7. He B, Nie Q, Wang F, et al. Role of pyroptosis in atherosclerosis and its therapeutic implications. *J Cell Physiol*. 2021;236(10):7159-7175. doi:10.1002/jcp.30366
8. Zhang Y, Liu X, Bai X, et al. Melatonin prevents endothelial cell pyroptosis via regulation of long noncoding RNA MEG3/miR-223/NLRP3 axis. *J Pineal Res*. 2018;64(2):e12449. doi:10.1111/jpi.12449
9. Liao K, Lv DY, Yu HL, Chen H, Luo SX; iNOS regulates activation of the NLRP3 inflammasome through the sGC/cGMP/PKG/TACE/TNF-alpha axis in response to cigarette smoke resulting in aortic endothelial pyroptosis and vascular dysfunction. *Int Immunopharmacol*. 2021;101(Pt B):108334. doi: 10.1016/j.intimp. 2021. 108334
10. Guo Y, Yang JH, He Y, et al. Protocatechuic aldehyde prevents ischemic injury by attenuating brain microvascular endothelial cell pyroptosis via lncRNA Xist. *Phytomedicine*. 2022;94:153849. doi:10.1016/j.phymed.2021.153849
11. Gu C, Draga D, Zhou C, et al. miR-590-3p Inhibits Pyroptosis in Diabetic Retinopathy by Targeting NLRP1 and Inactivating the NOX4 Signaling Pathway. *Invest Ophthalmol Vis Sci*. 2019;60(13):4215-4223. doi:10.1167/iovs.19-27825
12. Boström P, Wu J, Jedrychowski MP, et al. A PGC1-α-dependent myokine that drives brown-fat-like development of white fat and thermogenesis. *Nature*. 2012;481(7382):463-468. doi:10.1038/nature10777
13. Yu Q, Kou W, Xu X, et al. FNDC5/Irisin inhibits pathological cardiac hypertrophy. *Clin Sci (Lond)*. 2019;133(5):611-627. doi:10.1042/CS20190016
14. Colaianni G, Cinti S, Colucci S, Grano M. Irisin and musculoskeletal health. *Ann N Y Acad Sci*. 2017;1402(1):5-9. doi:10.1111/nyas.13345
15. Li RL, Wu SS, Wu Y, et al. Irisin alleviates pressure overload-induced cardiac hypertrophy by inducing protective autophagy via mTOR-independent activation of the AMPK-ULK1 pathway. *J Mol Cell Cardiol*. 2018;121:242-255. doi:10.1016/j.yjmcc.2018.07.250
16. Deng J, Zhang N, Chen F, et al. Irisin ameliorates high glucose-induced cardiomyocytes injury via AMPK/mTOR signal pathway. *Cell Biol Int*. 2020;44(11):2315-2325. doi:10.1002/cbin.11441
17. Wang H, Pei S, Fang S, et al. Irisin restores high glucose-induced cell injury in vascular endothelial cells by activating Notch pathway via Notch receptor 1. *Biosci Biotechnol Biochem*. 2021;85(10):2093-2102. doi:10.1093/bbb/zbab137
18. Pan JA, Zhang H, Lin H, et al. Irisin ameliorates doxorubicin-induced cardiac perivascular fibrosis through inhibiting endothelial-to-mesenchymal transition by regulating ROS accumulation and autophagy disorder in endothelial cells. *Redox Biol*. 2021;46:102120. doi:10.1016/j.redox.2021.102120
19. Zhang Z, Li S, Cui M, et al. Rosuvastatin enhances the therapeutic efficacy of adipose-derived mesenchymal stem cells for myocardial infarction via PI3K/Akt and MEK/ERK pathways. *Basic Res Cardiol*. 2013;108(2):333. doi:10.1007/s00395-013-0333-5
20. Song Y, Wang B, Zhu X, et al. Human umbilical cord blood-derived MSCs exosome attenuate myocardial injury by inhibiting ferroptosis in acute myocardial infarction mice. *Cell Biol Toxicol*. 2021;37(1):51-64. doi:10.1007/s10565-020-09530-8
21. Ismail-Beigi F, Craven T, Banerji MA, et al; ACCORD trial group. Effect of intensive treatment of hyperglycaemia on microvascular outcomes in type 2 diabetes: an analysis of the ACCORD randomised trial. *Lancet*. 2010;376(9739):419-430. doi:10.1016/S0140-6736(10)60576-4
22. Bai B, Yang Y, Wang Q, et al. NLRP3 inflammasome in endothelial dysfunction. *Cell Death Dis*. 2020;11(9):776. doi:10.1038/s41419-020-02985-x
23. Siasos G. Diabetes and Cardiovascular Disease. *Curr Pharm Des*. 2020;26(46):5909-5910. doi:10.2174/1381612826462012180909 01
24. Zhang J, Ma Y, Li W. Curcumin reduces inflammation in mice with the psoriasis model by inhibiting NLRP3 inflammatory bodies. *Cell Mol Biol (Noisy-le-grand)*. 2022;67(6):48-54. doi:10.14715/cmb/2021.67.6.7
25. Tang R, Xu J, Zhang B, et al. Ferroptosis, necroptosis, and pyroptosis in anticancer immunity. *J Hematol Oncol*. 2020;13(1):110. doi:10.1186/s13045-020-00946-7
26. Zhang L, Yuan M, Zhang L, Wu B, Sun X. Adiponectin alleviates NLRP3-inflammasome-mediated pyroptosis of aortic endothelial cells by inhibiting FoxO4 in arteriosclerosis. *Biochem Biophys Res Commun*. 2019;514(1):266-272. doi:10.1016/j.bbrc.2019.04.143
27. Vandanmagsar B, Youm YH, Ravussin A, et al. The NLRP3 inflammasome instigates obesity-induced inflammation and insulin resistance. *Nat Med*. 2011;17(2):179-188. doi:10.1038/nm.2279
28. Zheng Z, Yang X, Yu Q, Li L, Qiao L; LncRNA-MALAT 1 regulates cardiomyocyte scorching in diabetic cardiomyopathy by targeting NLRP3. *Cell Mol Biol*. 2021;67(6):213-219. doi: 10.14715/cmb/2021.67. 6.28
29. Li Q, Zhang M, Zhao Y, Dong M. Irisin Protects Against LPS-Stressed Cardiac Damage Through Inhibiting Inflammation, Apoptosis, and Pyroptosis. *Shock*. 2021;56(6):1009-1018. doi:10.1097/SHK.0000000000001775
30. Yue R, Zheng Z, Luo Y, et al. NLRP3-mediated pyroptosis aggravates pressure overload-induced cardiac hypertrophy, fibrosis, and dysfunction in mice: cardioprotective role of irisin. *Cell Death Discov*. 2021;7(1):50. doi:10.1038/s41420-021-00434-y
31. Miao P, Ruiqing T, Yanrong L, et al. Pyroptosis: A possible link between obesity-related inflammation and inflammatory diseases. *J Cell Physiol*. 2022;237(2):1245-1265. doi:10.1002/jcp.30627
32. Zhang Y, Liu W, Zhong Y, et al. Metformin Corrects Glucose Metabolism Reprogramming and NLRP3 Inflammasome-Induced Pyroptosis via Inhibiting the TLR4/NF-κB/PFKFB3 Signaling in Trophoblasts: Implication for a Potential Therapy of Preeclampsia. *Oxid Med Cell Longev*. 2021;2021:1806344. doi:10.1155/2021/1806344
33. Wang Y, Liu H, Sun N, et al. Irisin: A Promising Target for Ischemia-Reperfusion Injury Therapy. *Oxid Med Cell Longev*. 2021;2021:5391706. doi:10.1155/2021/5391706

Supplementary materials

Supplemental Figure 1. The protein expression of NLRP3 after overexpression treatment. (A) Western blot assay of NLRP3 in each group. (B) The mRNA level of NLRP3. (C) Semi-quantification of NLRP3 expression. Data are expressed as the means ± SEM; n = 5; **P* < .05.